Internal distances in short polyelectrolytes: A Monte Carlo study

Chava Brender and Meir Danino
Department of Physics, Bar-Ilan University, Ramat-Gan 52900, Israel
(Received 27 May 1993)

The new critical phenomenon of a coil-rod transition that was studied in our previous papers [J. Chem. Phys. **92**, 4468 (1990); **93**, 2736 (1990); **94**, 3213 (1991); **97**, 2119 (1992); J. Phys. Chem. **96**, 5553 (1992)] is investigated further. The family of physical statistical bonds is expanded. An important additional bond, the linear statistical bond, is introduced. Parameters based on internal distance investigations are proposed and these are used to analyze the Monte Carlo data. One of the most important parameters is the average probability for a linear statistical bond at a site on the chain, P_l. Indications are reported that scaling behavior in polyelectrolyte chains exists only for chain lengths having the same kink fraction g. An important relation is shown between the average number of kinks, $\langle n_{\text{kink}} \rangle$, and $D(2)$, the mean-square distance between the end beads of three adjacent beads in a cubic lattice: $g=\langle n_{\text{kink}} \rangle/N-2=1-[D(2)-2]/2=1-P_1$. In a previous article [J. Chem. Phys. **97**, 2119 (1992)] we found that for a self-avoiding-walk chain, g is constant and equal to 0.77. This relation leads to new constants, $P_1=0.23$ and $D(2)=2.46$ squared cell units in addition to the constant mean straight length $\langle l_s \rangle=1.29$ cell units, found in the above reference, to be connected to g. The large size effect that was found in this reference is also demonstrated here, i.e., segments of a small chain tend to expand less than segments of a long chain. The blob concept is examined and it is shown that all interior segments of the chain are stretched by repulsive interactions. This is inconsistent with the basic assumption of the blob concept. Howver, because the change in short segments of a chain is small when compared to the large change in long segments, the continued use of the blob concept remains valid for analytic estimations of the whole chain length. The polyelectrolyte expansion is extended to describe polymer expansion in general. An empirical relation is proposed between the mean-square radius of gyration $\langle S^2 \rangle$ and the mean-square internal distance between the ends of a half chain $D(N/2)$, and is expressed by $D(N/2)=3\langle S^2 \rangle$. An additional empirical relation is shown: $P_1=D(N/3)/(N/3)^2$ where $D(N/3)$ is the mean-square internal distance between the ends of one-third of the chain. Verification is found for the existence of the physical statistical bonds that vary with internal distance. The existence of these bonds is extended to various internal distances and to systems with various types of charge.

PACS number(s): 61.25.Hq, 05.70.Fh, 02.70.Lq, 02.50.Ng

I. INTRODUCTION

The great advantage that computer experimentalists have over scientists using other methods of analysis is the ability to obtain the specific coordinates of atoms in a molecular chain within the model framework. This permits a detailed analysis that was unachievable in the past. The ability to analyze atomic scales is comparable to some extent to the impact on biological research of the introduction of the electron microscope, which enabled one to see details that could only have been imagined previously. The closeup view of the polymer chain afforded by a computer analysis brings with it the possibility to define new parameters that disclose previously unknown characteristics of the chain.

Owing to these advances and to the availability of more powerful computers, the field of computer simulation and specifically the simulation of polyelectrolytes has developed considerably [1–41]. In previous articles [17,25,33,34], we dealt with the unfolding of a charged chain caused by physical changes in charge, temperature, salt concentration, or solvent. The salt concentration has been shown to diminish the unfolding process. In Refs. [25,33,34], we examined the extension mechanism of this intramolecular reaction using various parameters and found that the process exhibits characteristics of a phase transition. In this article, the analysis is extended using new parameters which are related to the previous parameters and which give new insight into chain behavior.

The model used and the simulation techniques are described in Sec. II. In Sec. III, the new parameters and new relations are introduced and the results are discussed. A summary follows in Sec. IV.

II. MODEL AND SIMULATION TECHNIQUE

The chain model to be discussed here is the same as in Ref. [17(a)]. A fully charged chain with equally distributed charge is represented by N hard spherical beads of diameter $d=4$ Å in a cubic box. The box has a length of 2048 Å and satisfies periodic boundary conditions. This model is based on the Lax-Brender-Windwer (LBW) model modified by ideas introduced by Carnie *et al.* [14(a)]. The Coulomb potential is replaced by the screened Debye-Hückel (DH) potential, which mimics an "added salt." There are two cases: the bare chain having concentration $C=0M$ (no added salt) and the DH screened chain with $C\neq 0M$ (added salt). To avoid lengthiness, we discuss in this article only the bare chain. The case of added salt will be considered in a separate ar-

ticle. Monte Carlo (MC) simulations were carried out on an IBM 3090 computer at Bar-Ilan University for chain lengths between 8 and 64 beads for various values of an independent parameter λ, defined [17(a)] as z^2e^2/DkT, where z is the charge on each ion of the chain and D is the dielectric constant of the solvent. At room temperature for a polyelectrolyte in water solution, $\lambda=7.14$ Å. Ensemble averages were collected after rejecting the initial cycles before relaxation. Subsequent groups of 10 000 cycles were averaged separately and then averages and standard deviations of the means over all groups were calculated. A total number of 1 800 000 cycles were generated for each set of simulated experimental conditions. For further description of the computational technique, see Refs. [17(a),33,34].

III. PARAMETER DEFINITIONS, RESULTS, AND DISCUSSION

A commonly used parameter in polymer physics is the mean-square end-to-end distance R^2. A similar parameter is the mean-square distances between any of the polymer chain beads. We denote by $D(n)$ the mean-square end-to-end distance of all subchains consisting of n links in a chain of N beads. For example, $D(2)$ is the mean-square distance of two links, or, in other words, the end-to-end distance of three adjacent beads in a chain of N beads. We denote it also as an internal end-to-end distance to distinguish it from the external end-to-end distance. After averaging over all possibilities in a single polymer configuration, an average was calculated in a way similar to the other averaged parameters as described in Sec. II and in Ref. [17(a)]. An average of $D(n)$ over a group of 10 000 configurations was obtained, after which an average over 180 groups was calculated.

Values were calculated of the vectors $D(n)$, where n is varied from 2 to $N-1$. Listed in Tables I and II are the values of $D(2)$, which describe the mean-square distances between bead i and bead $i+2$, and the values of $D(3)$, which describe the mean-square distances between bead i and $i+3$.

In this article, we emphasize the internal square distances $D(2)$, and also discuss $D(3)$ and distances where $n \geq 4$. Also, from a chemical point of view $D(2)$ and $D(3)$ are of great significance because neighboring beads may participate in a mutual chemical reaction. The mean-square distance between beads 1 and N, $D(N-1)$, is usually denoted as the mean-square end-to-end distance of a chain of N beads. It is of interest to compare the behavior of the internal distances with that of the end-to-end distance. Therefore, in Fig. 6, we have plotted several of the internal and end-to-end square distances on the same graph for comparison.

We first consider $D(2)$, the mean-square distance between beads i and $i+2$ in a polymeric chain. The connectivity of three beads in a self-avoiding-walk (SAW) chain on a cubic lattice is possible in two configurations: (i) a bend configuration (kink), which is shown in Fig. 1(a), and (ii) a straight connection, which we denote as a *linear statistical bond* and which is shown in Fig. 1(b). The mean-square distance between bead i and bead $i+2$ equals two square units for a kink and four square units for the straight connection. Four square units is therefore, by definition, the maximum theoretical value of $D(2)$ in a cubic chain and two square units is the minimum theoretical value. The calculated values of $D(2)$ must lie between these two limiting values. This is indeed what we observe from our MC calculations of $D(2)$ for polyelectrolyte chains and is summarized in Table I. The following paragraphs discuss what has been learned from the study of the values of the internal distances using the $D(n)$ parameter.

TABLE I. Values of $D(2)$, the mean-square distance between bead i and bead $i+2$ (in cell units), for various polyelectrolyte chain lengths N, and various λ at $C=0M$.

λ	$N=8$	$N=16$	$N=32$	$N=48$	$N=64$
0	2.42	2.44	2.44	2.45	2.46
1	2.50	2.58	2.64	2.69	2.72
2	2.58	2.70	2.83	2.90	2.96
3	2.66	2.83	3.04	3.20	3.26
4	2.74	2.97	3.25	3.40	3.50
5	2.82	3.08	3.40	3.60	3.64
6	2.89	3.21	3.60	3.70	3.76
7	2.97	3.35	3.70	3.80	3.83
8	3.04	3.47	3.73	3.83	3.88

A. Local size effect

From Table I, it is seen that for $\lambda=0$, the values of $D(2)$ are almost identical for all values of N, being slightly greater for higher N, in the range $N \leq 64$. In Sec. III H we discuss this phenomenon, which occurs for all $D(n)$. As λ increases, values of $D(2)$ increase. This is consistent with the extension of the chain discussed in Ref. [17(a)]. Moreover, as λ increases, there is an increase in the differences between values of $D(2)$ for various chain lengths. For example, there is a difference of 0.04 between the values of $D(2)$ for $N=64$ and $N=8$ at $\lambda=0$. At $\lambda=7$, the difference is 0.86. It follows that the local expansion with increasing λ is greater at high N. The expansion is denoted as local because it describes the minimum possible square distance between unconnected beads. This local size effect, which is quite pronounced at high λ, is consistent with the global size effects described in Ref. [34], according to which a small chain tends to ex-

TABLE II. Values of $D(3)$, the mean-square distance between bead i and bead $i+3$ (in cell units) for various polyelectrolyte chain lengths N, and various λ at $C=0M$.

λ	$N=8$	$N=16$	$N=32$	$N=48$	$N=64$
0	4.1	4.1	4.1	4.2	4.2
1	4.3	4.6	4.8	5.0	5.1
2	4.6	5.0	5.4	5.6	5.8
3	4.8	5.4	6.0	6.5	6.8
4	5.1	5.8	6.7	7.1	7.4
5	5.3	6.3	7.2	7.7	7.9
6	5.6	6.6	7.7	8.1	8.3
7	5.8	7.0	8.0	8.3	8.5
8	6.0	7.4	8.3	8.5	8.7

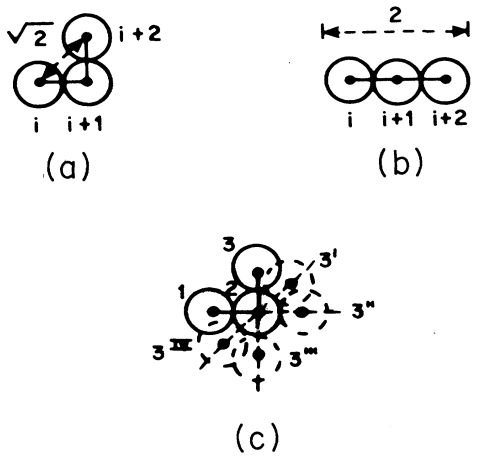

FIG. 1. Three connected beads i, $i+1$, and $i+2$ (a) in a bend configuration and (b) in a linear configuration. The distance between the extreme beads is denoted by dotted lines. (c) A short chain of three beads. The four dashed circles are alternative sites for bead number 3 on the cubic lattice.

pand less than a long chain. This tendency of the small chains is attributed mainly to the proximity of all the beads of the small chain to the end beads [34,26]. In their recently published article, Lai and Binder [42] found that under the same shear flow, longer grafted polymer chains are more stretched than short chains (Fig. 5 in Ref. [42]). This shows that there is a generalized characteristic which is the same whether attributed to charge, shear flow, or other causes. A connection between $D(2)$ and the kink fraction g was found (see Sec. III C 1) and therefore it is to be expected that the size effects that were found through the kink fraction [34] appear here as well.

B. New parameter P_l: The average probability for a linear statistical bond at a site on the chain

The parameter $D(2)$ can be used to calculate other important parameters, for example, P_l, *the average probability for the existence of a linear bond.* The average square distance $D(2)$ between bead i and bead $i+2$ is actually the sum of the square distance, 4, of the linear bond multiplied by its probability P_l and the square distance, 2, of a kink multiplied by its probability $1-P_l$. Thus

$$4P_l+2(1-P_l)=D(2)\ . \tag{1}$$

Solving this equation for P_l, we obtain

$$P_l=[D(2)-2]/2\ . \tag{2}$$

Substituting $D(2)=2.46$ for $N=64$ at $\lambda=0$, we find

$$P_l=0.23\ .$$

This means that 23% of the three connected beads, i, $i+1$, and $i+2$, in a SAW chain of $N=64$ beads (at $\lambda=0$) are arranged linearly, as shown in Fig. 1(b). The remaining 77% are bent as shown in Fig. 1(a). In a cubic lattice, of course, the only possibilities are a straight line or one bend by 90°. Values of P_l, the average probability for a linear statistical bond at a site on the chain for various λ and different values of N, were calculated using Eq. (2), and are shown in Fig. 2. It is interesting to note that at $\lambda=0$, all N have almost a constant value of $P_l=0.23$.

As λ increases, the values of P_l for various N increase in different manners. For large N they increase "faster" than for small N. $N=8$ and $N=16$ are separated while $N=32$, 48, and 64 are close together. The large size effects found for g in Fig. 8 of Ref. [34] appear for P_l as well. This points to a possible connection between the two parameters. In Sec. III C we discuss this connection. It is important to add that in contrast to contacts and kinks, the linear statistical bonds increase with λ. This increase is described in Fig. 2 and is caused by the decrease in the number of kinks. Owing to chain connectivity, the disappearance of a kink in a chain causes the creation of a linear bond. This is the reason that we denote P_l also as the *unkink probability.*

It is easy to see from Fig. 1(c) that in a cubic lattice for $N=3$, bead 3 has five possible configurations (four kinked and one linear). The unkink probability P_l for this short chain of $N=3$ beads is 1 in 5, or $P_l=0.2$. At larger N, P_l should be a bit higher because of excluded volume, i.e., at higher N there is a slightly greater tendency of each bead to distance itself from the others. This explains the value of $P_l=0.23$ found by the MC numerical method shown above. Similar arguments were given as explanation for the mean straight length $\langle l_s \rangle$ larger than 1.2 in Ref. [33]. The existence of a fixed value of $P_l=0.23$ (for a SAW chain) above a certain N means that when the only limitations are excluded volume, the polymer chain finds its own ratio of kinks to linear bonds and these proportions are maintained for any chain length.

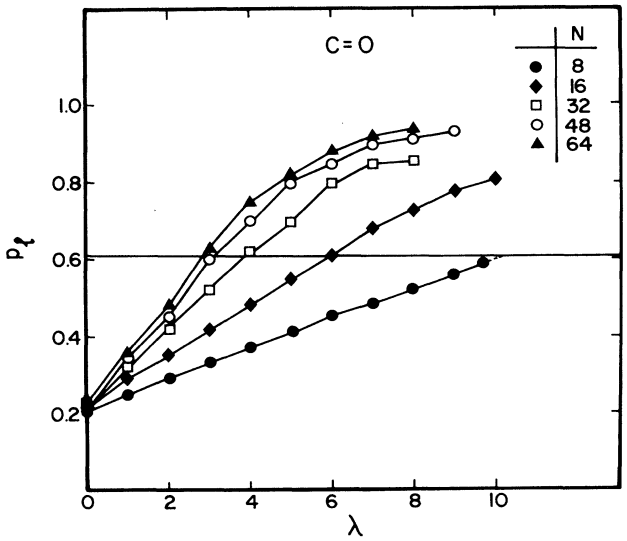

FIG. 2. P_l, the average probability for a linear statistical bond at a site on the chain (also denoted as the unkink probability), vs λ (Å) for a bare polyelectrolyte ($C=0M$), for chains of various N. The horizontal line at $P_l=0.61$ intersects the curves at a λ denoted as $\lambda_{1/2}$ [48], which is observed to vary at different chain lengths (in the investigated range). The curves have been drawn to guide the eye.

C. Kink probability

1. New relations

The probability P_l for a linear statistical bond at a site on the chain is complementary to the probability for a kink, which is therefore $1-P_l$. Multiplying the probability to find a kink, $1-P_l$, by $N-2$ (the maximum number of kinks available in a chain of N beads [34]) gives the average number of kinks, $\langle n_{\text{kink}} \rangle$, i.e.,

$$(1-P_l)(N-2)=\langle n_{\text{kink}} \rangle \ . \tag{3}$$

Thus

$$1-P_l=\langle n_{\text{kink}} \rangle /(N-2) \ , \tag{4}$$

which is the definition of the kink fraction g, defined in Ref. [34] as

$$g=\langle n_{\text{kink}} \rangle /(N-2) \ . \tag{5}$$

Thus

$$1-P_l=g \ . \tag{6}$$

Equation (6) adds new meaning to the kink fraction g defined in Ref. [34], namely, the probability for the existence of a kink at a site along the chain. The kink probability $1-P_l$ is derived from $D(2)$ [Eq. (2)], while the kink fraction g is derived from the average number of kinks $\langle n_{\text{kink}} \rangle$ divided by $N-2$. Table III gives a comparison of the calculated values of $1-P_l$ at various λ, for various N and values of g, where $\langle n_{\text{kink}} \rangle$ was measured directly. The similarity of the results calculated by two different methods gives support to the self-consistency of our calculations. Identifying $1-P_l$ as g helps to clarify the connection between $\langle n_{\text{kink}} \rangle$ and $D(2)$. This implies a connection between local $[D(2)]$ and overall $[\langle n_{\text{kink}} \rangle]$ parameters:

$$\langle n_{\text{kink}} \rangle /(N-2)=1-[D(2)-2]/2 \ . \tag{7}$$

Equation (7) is actually a combination of Eqs. (2) and (4). From (7), it follows that in the straight rod, when $D(2)=4$, the average number of kinks is 0, and in the case of a coil, for $N=64$ where $D(2)=2.46$ square units, $g=0.77$. The same result was reported in Ref. [34], using a different method of calculation. The connection between $D(2)$ and g explains the appearance of the large size effects described in Sec. III A, and first described for g in Ref. [34]. Because g is connected to the mean straight length $\langle l_s \rangle$ through Eqs. (2) and (4) of Ref. [34], it follows that for a cubic lattice SAW chain, the universal values of $\langle l_s \rangle=1.29$ cell units, the constant value of $g=0.77$ [34], the constant value of $P_l=0.23$, and also the value of $D(2)=2.46$ square units, that are found in this section, are all connected to each other. Thus, from Eq. (7), a constant value of g at $\lambda=0$ [34] implies a new constant value for $D(2)$. The mean-square distance $D(2)$ between bead i and bead $i+2$ of a SAW chain thus seems to equal 2.46 square units. For the simple case of $N=3$ of Fig. 1(c), where there exist four kinks and one linear bond, $D(2)$ can be calculated exactly and is given by $(4\times2+4)/5=2.4$ square units. For chains with higher N due to excluded volume, the proportions between linear bond and the total number of possible configurations has been shown (Sec. III A) to be 0.23, which is larger than 1:5. Therefore $D(2)$ should be a bit greater than 2.4, as we indeed found.

2. Remarks on the blob assumption

The new relation between $D(2)$ and g [Eq. (7)] is valid not only when g is constant but also when g varies with λ. In Fig. 8 of Ref. [34], we showed how g varies with λ. Equation (7) clearly shows that changing g is equivalent to varying $D(2)$. These results allow us to question, in such systems, the basic assumption behind the blob concept. According to this concept, inside a blob the chain is nearly ideal and between blobs there are strong repulsions [44–46]. Table I and Fig. 3 show that even the values of $D(2)$, the shortest mean-square internal distance, do not maintain a constant value for changes in λ. Changes in $\langle l_s \rangle$ were recorded (see Table VI and the discussion in Ref. [33]) even for $0 \le \lambda \le 1$, the range where the blobs would be most likely to exist according to Ref. [46]. Since g and $\langle l_s \rangle$ are connected through Eqs. (2) and (4) of Ref. [34], changes in $\langle l_s \rangle$ imply changes in g when λ increases.

Our results show no evidence that the changes in average values of square distance are caused only by changes

TABLE III. Comparison of g and $1-P_l$. Values of $1-P_l$ calculated from values of $D(2)$ using Eq. (2). Values of g, the kink fraction, are calculated from the expression $\langle n_{\text{kink}} \rangle /(\langle n_{\text{kink}} \rangle + \langle n_{\text{linear}} \rangle)$, where $\langle n_{\text{kink}} \rangle$ is the average number of kinks in a polyelectrolyte chain directly measured [43] and $\langle n_{\text{linear}} \rangle$ is the average number of linear bonds.

	$N=8$		$N=16$		$N=32$		$N=48$		$N=64$	
λ	$1-P_l$	g	$1-P_l$	g	$1-P_l$	g	$1-P_l$	g	$1-P_l$	g
0	0.79	0.79	0.78	0.78	0.78	0.78	0.78	0.78	0.77	0.77
1	0.75	0.75	0.71	0.72	0.68	0.68	0.66	0.66	0.64	0.64
2	0.71	0.71	0.65	0.65	0.59	0.58	0.55	0.54	0.52	0.51
3	0.67	0.67	0.59	0.58	0.48	0.49	0.40	0.41	0.37	0.37
4	0.63	0.63	0.52	0.52	0.38	0.39	0.30	0.31	0.25	0.26
5	0.59	0.59	0.45	0.45	0.30	0.30	0.20	0.22	0.18	0.18
6	0.56	0.56	0.40	0.38	0.20	0.22	0.15	0.17	0.12	0.12
7	0.52	0.52	0.32	0.32	0.15	0.17	0.10	0.11	0.08	0.09
8		0.48		0.27		0.12		0.08		

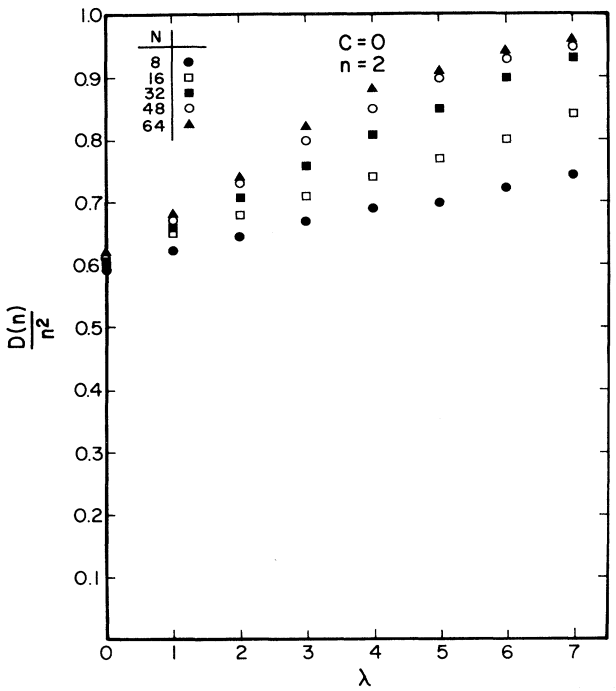

FIG. 3. Values of normalized mean-squared internal distances (in cell units) $D(2)/2^2$ vs λ (Å) for a bare polyelectrolyte chain ($C=0M$), for various number N of chain beads.

between blobs and are not distributed over the entire chain. The Monte Carlo results support our belief that in polymers all beads are equally free to move. As the chain expands, the blob assumption implies that the expansion occurs only between the blobs, but inside a blob the chain remains unchanged in its SAW configuration. The assumption that the expansion is not distributed among all beads but only between blobs is equivalent to discrimination between beads, which we feel is against the inherent justice embedded in scientific laws.

3. P_{li}, the unkink probability for each group of three beads

To verify that expansion is distributed along the entire chain, we calculated P_{li}, *the unkink probability for each group of three beads* in a chain of $N=16$ for various values of λ. This was done by counting the average number of linear statistical bonds in each configuration for each three-bead segment of the chain using the same procedure described for the other configurational properties. The results are shown in Table IV and Fig. 4. The table clearly shows that as λ is varied, there are changes in P_{li} for every three adjacent beads in the chain. The amount of extension varies along the length of the chain, with beads near the ends extending less than beads near the center. The markers in Fig. 4 show that for $\lambda=0$ all chain beads have the same value of P_{li} (except for the end beads, which have slightly lower values of P_{li}). As λ increases, for low λ, the extension is close to linear, while at higher λ the extension of the center of the chain is much greater than near the ends. The result, that the ends remain relatively bent while the middle tends to straighten out, was mentioned in Refs. [25,34] and is in agreement with Rabin's conclusions [47] for polymer conformation in elongational flow. Note that there exists a large difference between the middle of the chain and the ends at high λ. For $N=32$ the middle of the chain is higher and flatter and the average P_l is higher (less influenced by the end beads). Note also that the column of P_l in Table IV has values that correspond to the values of the $1-P_l$ column for $N=16$ in Table III, which supports the consistency of our calculations. Note also that all values of the P_l column in Table IV resemble the 3–5 column of P_{li} as if the linear probability of bead no. 4 in the chain of 16 beads is representative of the whole chain (bead no. 1 is located at one of the chain ends). The same occurs to the chain of $N=32$ beads, but the representative bead of the chain is bead no. 7. For $N=48$ the representative is bead no. 8; for $N=64$ it is bead no. 11 for $\lambda<5$; and for $\lambda\geq 5$ bead no. 9; and for $N=8$ it is bead no. 3. These bead numbers reflect the influence of the chain ends, which is higher for lower N.

4. Further remarks on the blob assumption

Simulations on the atomic scale can check assumptions on which analytical models are based. In this context it

TABLE IV. Values of P_{li}, the unkink probability, for each group of three beads in a polyelectrolyte chain of 16 beads, at various λ. For example, the column titled 7–9 gives the probability for a linear statistical bond between beads 7, 8, and 9. The column titled P_l gives the average unkink probability calculated from the values of P_{li} of the groups of the chain in each row.

		P_{li}													
λ	P_l	1–3	2–4	3–5	4–6	5–7	6–8	7–9	8–10	9–11	10–12	11–13	12–14	13–15	14–16
0	0.225	0.209	0.222	0.223	0.224	0.236	0.227	0.234	0.230	0.232	0.231	0.226	0.225	0.217	0.211
0.5	0.258	0.224	0.241	0.260	0.260	0.266	0.275	0.276	0.279	0.275	0.273	0.267	0.257	0.243	0.220
1	0.291	0.232	0.269	0.289	0.297	0.309	0.315	0.313	0.321	0.318	0.312	0.303	0.288	0.266	0.239
1.5	0.325	0.251	0.293	0.329	0.341	0.349	0.360	0.357	0.361	0.358	0.353	0.341	0.323	0.289	0.251
2	0.356	0.260	0.318	0.352	0.376	0.390	0.402	0.406	0.400	0.390	0.386	0.373	0.355	0.317	0.257
2.5	0.390	0.278	0.352	0.382	0.412	0.429	0.432	0.443	0.442	0.434	0.427	0.415	0.388	0.346	0.278
3	0.424	0.286	0.368	0.420	0.446	0.468	0.487	0.492	0.487	0.485	0.468	0.450	0.416	0.370	0.293
4	0.490	0.316	0.413	0.477	0.523	0.549	0.567	0.586	0.588	0.570	0.554	0.521	0.470	0.414	0.319
5	0.549	0.345	0.464	0.544	0.596	0.625	0.639	0.649	0.643	0.626	0.609	0.582	0.542	0.467	0.351
6	0.600	0.377	0.521	0.614	0.678	0.709	0.746	0.766	0.770	0.751	0.722	0.668	0.609	0.511	0.366
7	0.680	0.395	0.567	0.664	0.737	0.779	0.805	0.805	0.809	0.808	0.789	0.752	0.687	0.580	0.404
8	0.747	0.433	0.608	0.738	0.812	0.853	0.877	0.900	0.894	0.879	0.862	0.819	0.740	0.608	0.434

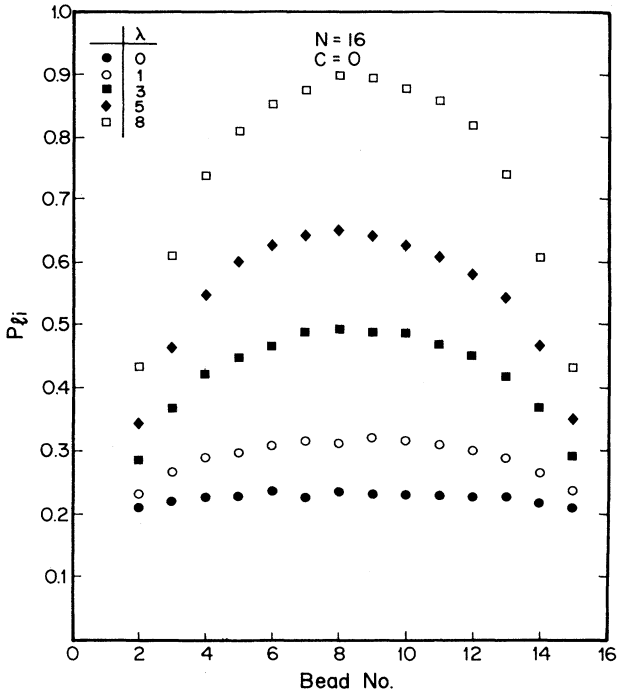

FIG. 4. Values of P_{li}, the unkink probability, at various values of λ (Å) for each three-bead segment of a polyelectrolyte chain of 16 beads. The bead numbers indicate the middle bead of the segment. (E.g., segment 3–5 is denoted as bead no. 4). The values are taken from Table IV.

is important to note that our numerical simulations do not assume the existence of blobs as a basis for calculations. The justification for the argument that the monomers inside a blob remain unchanged may possibly be found by considering a long chain relative to its short segments. Because each blob contains several monomers, naturally the mean-square distance over a group of blobs is $D(n)$, where n is large. The MC results of $D(n)$ for low n and high n are compared in Fig. 6 and discussed in Sec. III D. We note here that for higher values of n, the markers of $D(n)/n^2$ have higher slopes. Therefore the change in $D(2)$, the smallest possible blob, may be negligible when compared to the change in $D(10)$, for example. This is similar to the assumption made in the blob hypothesis. When there is a need for greater accuracy in analytic estimates, the results may be improved by substituting a slightly larger value for the length of each blob calculated numerically. When examining a short segment of the chain, the blob hypothesis is not applicable and numerical methods are preferable.

In their recent article, Barrat and Boyer [37] discuss internal distances and blobs in a clear manner. In comparing our model with theirs, it should be noted that, as they mention, their model does not take into account the short-range excluded-volume effects. This is especially important in comparing internal distances of short segments. The value of their coupling parameter $u=0.1$ is equivalent to our $\lambda=0.4$ Å, since $u=\lambda/d$ and our $d=4$ Å. The condition $\lambda=0.4$ Å is close to $\lambda=0$, which is the condition for a SAW chain.

Barrat and Boyer base their Eq. (23) on the assumption that the chain is a linear string of blobs, as in Fig. 1 of Ref. [46]. In view of our results [25,48], which are limited to $N \leq 64$, this assumption cannot be confirmed for the description of such a weakly charged molecule. Even in terms of the results listed in their Table I, the significance of the blob concept appears dubious. For the SAW limit, $u \rightarrow 0$, the blob is the size of the entire chain. For $u \rightarrow 0.5$ the blob approaches the size of the monomer. Thus the possible values of u for blob use are severely limited and, even in this limited range, the assumption of a linear string of blobs is not justified enough.

D. *Normalized* internal squared distances

It is difficult to compare values of $D(n)$ for various n on the same plot. This difficulty can be overcome by using the *normalized values of* $D(n)$, i.e., $D(n)$ values divided by the maximum possible expansion n^2. In Figs. 3 and 5, respectively, we plot $D(2)/4$ and $D(3)/9$, the "normalized internal distances" of $D(2)$ and $D(3)$ for various chain lengths. The values of $D(n)/n^2$ fall naturally between zero and unity. A value close to unity denotes almost a straight line configuration and a low value denotes high coiling. This implies that the parameter $D(n)/n^2$ may be considered as an inverse measure of the flexibility. It is seen from Figs. 3 and 5 that as λ increases, the values of $D(n)/n^2$ increase. That is, the flexibility decreases when the chain straightens out into a rod.

It is interesting to note that over the investigated range

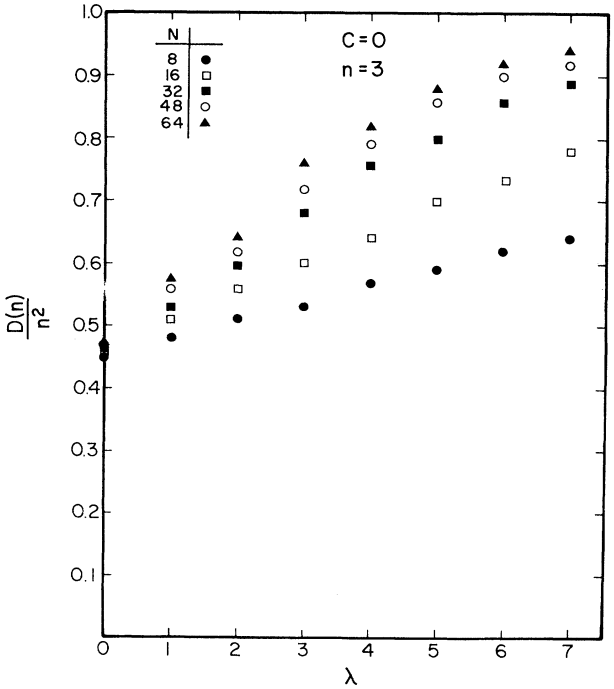

FIG. 5. Values of normalized mean-squared internal distances (in cell units) $D(3)/3^2$ vs λ (Å) for a bare polyelectrolyte chain ($C=0M$), for various number N of chain beads.

of λ, $D(2)/4$ (Fig. 3) varies from ~ 0.6 to ~ 1, while $D(3)/9$ (Fig. 5) varies from ~ 0.4 to ~ 1. The difference in this range of values reflects the difference in flexibility caused by a single additional bead being involved in the internal segments of the chain whose end-to-end distance is investigated. The flexibility parameter (for $\lambda=0$) clearly stresses the advantage of a long chain over a short chain, namely, that long chains can be arranged in more geometrical configurations than short chains, thus gaining higher entropies. This is true for the entire chain as well as for its internal segments.

The large size effect, pointed out in Ref. [34] and in the discussion of the data of Tables I and II, is also seen in Figs. 3 and 5. The values of $D(n)/n^2$ are close together for various N at $\lambda=0$, while at $\lambda\neq 0$ the values of $D(n)/n^2$ for long chains are higher than those for short chains. Because n is the same in these figures for all N, the differences in $D(n)/n^2$ stem from the values of $D(n)$, which was found in Tables I and II to have large size effects. This indicates that long chains at $\lambda\neq 0$ are less flexible than short chains, as was already shown in Ref. [34], using the parameter g. These differences in flexibility with chain length at $\lambda\neq 0$ may be the reason for the failure of the scaling theory to yield the same value for the exponent with different chain lengths in this regime of N [21,49].

This idea, together with the idea that at $\lambda=0$ scaling is known to be valid, implies that g (or P_l) has a unique value. Values of $\ln\langle S^2\rangle$ vs $\ln N$ for chains with $P_l=0.61$ were plotted. The values for $\langle S^2\rangle$ were taken at points of λ for which $P_l=0.61$ intersects the curves in Fig. 2, and similarly for $P_l=0.50$ and 0.40. The plots are not included in this article since the data is incomplete, but it is important to report here that straight lines were formed.

This indicates that for identical g or P_l, scaling is valid, and polymer chains with different g's have different exponents. Further investigation of this issue is planned.

Note that $D(3)$ at $\lambda=0$ (SAW chain) seems to attain a constant value of 4.2 (see Table II and Fig. 8). The significance of $D(3)$ will be discussed in a future article.

The differences between the values of $D(n)/n^2$ for various values of n in a chain of N beads become clearer from Fig. 6 where values of $D(n)/n^2$ for various internal segments n are depicted for a chain of $N=32$ beads. One observes that the "starting" values at $\lambda=0$ are smaller for longer segments, i.e., larger flexibilities for long SAW subchains, and that all $D(n)/n^2$ values increase as λ increases. It is easy to compare from Fig. 6 the normalized values of $D(2), D(3), \ldots, D(n)$. Small n have higher normalized values for the whole range of λ, which implies lower flexibilities. The variance in these normalized values with λ is also interesting. It seems that the higher values of n have larger slopes, indicating that *large values of n are more sensitive to changes in λ than small values of n.* The idea that changes due to physical conditions (λ) are small for short segments and large for long segments is reminiscent of the butterfly effect in chaos.

It is also clear from Fig. 6 that all $D(n)/n^2$ increase gradually as λ increases. There exists no normalized internal square distance for any value of n that is not affected by λ.

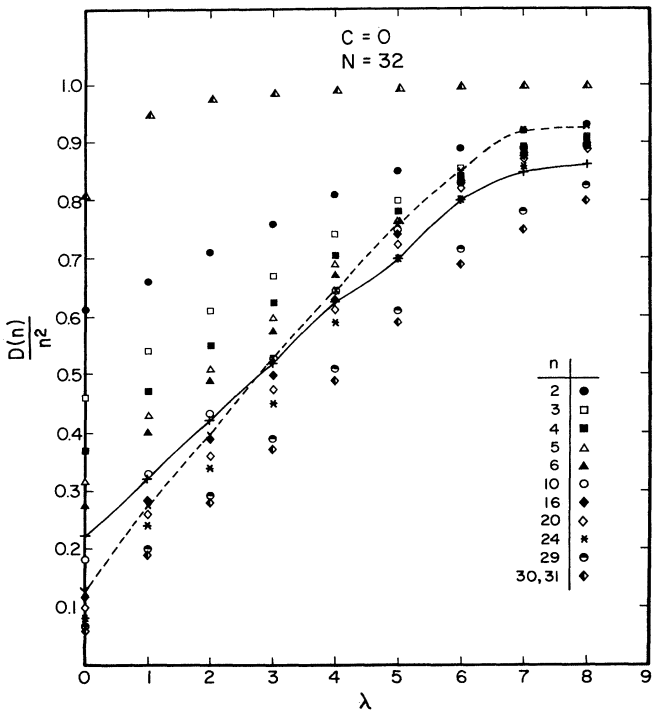

FIG. 6. Values of various normalized mean-squared internal distances (in cell units) $D(n)/n^2$ vs λ (Å) for a chain of $N=32$ beads, for a bare polyelectrolyte chain ($C=0M$). The half-filled triangles denote values of the uncontact probability P_{nc} calculated from values of the average number of contacts $\langle n_t\rangle$ [25], using Eq. (9). $\times$ denotes values of $\langle S^2\rangle/\frac{1}{12}(N-1)^2$. A dashed line has been drawn to guide the eye. $+$ denotes values of P_l [calculated from the values of $D(2)$ using Eq. (2)]. A solid line has been drawn to guide the eye.

E. Contact fraction and the uncontact probability

Similarly to the kink fraction g, we can define the contact fraction g_c:

$$g_c=\langle n_t\rangle/(N-3)\ , \tag{8}$$

where $\langle n_t\rangle$ is the average number of all types of contacts in a polymer chain [25] and $N-3$ is the maximum number of contacts in the chain.

Similarly, regarding the relation between P_l and g, we can define P_{nc}, the uncontact probability, i.e., the probability of not having a contact in a chain.

$$P_{nc}=1-\langle n_t\rangle/(N-3)\ . \tag{9}$$

In Fig. 6, we plot P_{nc} calculated using Eq. (9) from the values of $\langle n_t\rangle$ for a chain of $N=32$ beads [25], for various values of λ. From the figure one can observe that the values of P_l and $\langle S^2\rangle/\frac{1}{12}(N-1)^2$ are close to each other (especially for $\lambda\geq 1$). The values of P_{nc} located at the top of the figure are very different from the values of P_l, which indicates that $\langle S^2\rangle/\frac{1}{12}(N-1)^2$ is very different from P_{nc}. (Note that the values of P_{nc} are closer to unity than any of the P_l values.)

This difference in the values between these parameters

also suggests that $\langle S^2 \rangle$ is influenced by P_l (or g), which is connected to the average number of linear bonds (or their complementary quantity, $\langle n_{\text{kink}} \rangle$), and not by the average number of contacts. This result supports the similar result obtained by a different method (salt sensitivity) in Ref. [34]. In fact, we have already proved this numerically and plan to discuss it in a future article.

F. New relation between $D(N/2)$ and $\langle S^2 \rangle$

Figure 6 shows values for normalized parameters $D(N/2)$ and $\langle S^2 \rangle$. It is surprising to find that the markers of the two parameters are close to each other. $\langle S^2 \rangle$ is normalized by dividing $\langle S^2 \rangle$ by the maximum mean-square radius of gyration of a rod, i.e., for $N=32$ by dividing $\langle S^2 \rangle$ by $\frac{1}{12}(31)^2$. The normalized $\langle S^2 \rangle$ values are close to the markers of $D(16)/16^2$. We found the same phenomenon for a charged chain of $N=48$ (not shown). This indicates proportionality between the values of $\langle S^2 \rangle$ and $D(n)$ when n equals half the number of beads ($n=N/2$). This interesting relation is described further in Fig. 7.

Values of the ratio $D(N/2)/\langle S^2 \rangle$ are shown in Fig. 7 for various chain lengths N at various λ. It is clearly seen that for the given range of N and λ, there is an almost fixed ratio of 3:1 between the two parameters. Thus, from the Monte Carlo simulations of polyelectrolytes, it is found empirically that for $0 \le \lambda \le 8$, $N \le 64$,

$$D(N/2)=3\langle S^2(N) \rangle \ . \tag{10}$$

It is interesting to note that the average value of the ratio $\langle S^2 \rangle / \langle R^2 \rangle$ decreases from $\frac{1}{6}$ to $\frac{1}{12}$ with increasing λ (as can be seen in Table III of Ref. [17(a)]). This is in contrast to the ratio $D(N/2)/\langle S^2 \rangle$, which remains constant with increase of λ, as observed from Fig. 7.

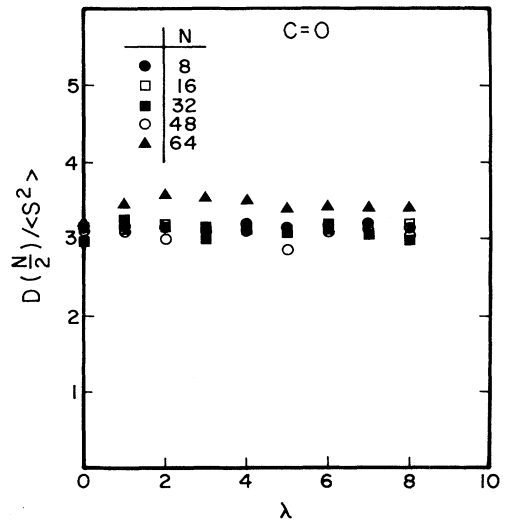

FIG. 7. Values of mean-squared internal distance of half-chain divided by the mean-square radius of gyration of the chain, vs λ (Å) for various N chain beads, for a bare polyelectrolyte ($C=0M$).

G. Proportionality between P_l and $D(N/3)$

Values of P_l calculated from Eq. (2) are also plotted for $N=32$ in Fig. 6. These values are close to the values of $D(10)/100$ also shown in Fig. 6. The same calculations were made for $N=48$ and $N=64$ and values of P_l were found to be close to the values of $D(n)/n^2$, where $n=N/3$.

An additional empirical relation is thus derived from the simulations.

$$P_l=D(N/3)/(N/3)^2 \tag{11}$$

for $0 \le \lambda \le 8$ and $N \le 64$.

It must also be added that the values for $D(2)/4$ for $N=32$ in Fig. 6 lie on a straight line for values of λ between 0 and 5. All the $D(n)/n^2$ values for $n>2$ have a higher slope from $\lambda=0$ to $\lambda=1$. For $1 \le \lambda \le 5$ and $2<n \le 20$, straight lines are observed. (Note that these results may be changed when $N \neq 32$). It is also observed from this figure that the values of $D(n)/n^2$ for n other than the extreme values (i.e., $n \neq 2,29,30,31$) converge around $\lambda=8$ and the ratio $D(n)/n^2$ takes an almost fixed value at this λ.

H. Values of $D(n)$ at $\lambda=0$ (neutral chain)

Although this article deals with charged chains, it is interesting to look at the plot of the mean-squared distance $D(n)$ for various chain lengths N for uncharged chains (SAW chains, $\lambda=0$) shown in Fig. 8. Because the values of $D(n)$ here are not normalized, it is possible to show only a few members of the family of $D(n)$ on the same scale. The $D(n)$ of a specific n may be an internal distance in one case, and an end-to-end distance in another case. For the case of $D(7)$ in a chain of $N=8$ beads, it is exactly the mean-squared end-to-end distance. For $N=32$ beads, $D(7)$ is an internal mean-squared distance. The two cases have different values for $D(7)$ because the excluded volume is different in each case. The excluded volume, when $D(7)$ is an internal distance, is greater than when it is an end-to-end distance, because near the end there is less steric hindrance. The value of $D(7)$ in a chain of $N=8$ chain beads is therefore smaller than for $N=16$ chain beads, and this is smaller than for $N=32$, as can be seen from Fig. 8.

The transition from an internal distance to an end-to-end distance causes a sharp decrease in the value of $D(7)$ when N is decreased to $N=8$. Despite the fact that for $N=8$, $D(6)$ is internal, we can observe the same behavior described above for $D(7)$: a sharp decrease when N is decreased to $N=8$. The reason is similar, because $D(6)$ constitutes most of the chain and for such distances, the chain already is close to the ends. It is probable that when N is three or four times larger than n, the $D(n)$ may be considered as an internal distance. This may be the cause for the difference in the values of $D(8)$, $D(9)$, and $D(10)$ between $N=32$ and $N=48$.

It is interesting to note that $D(2)$ is less sensitive to changes in N. This can be seen from the flat curve of $D(2)$ in Fig. 8. This may be caused by the fact that this three-bead square distances plays the role of an internal distance even for $N=6$, the lowest N considered in this

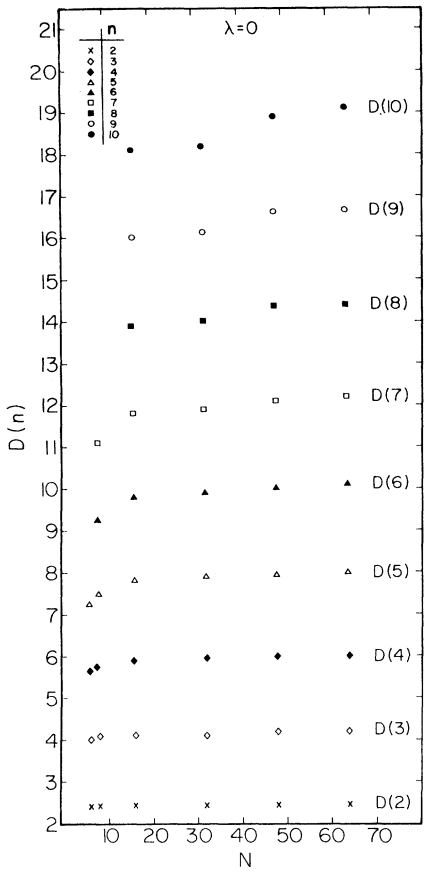

FIG. 8. Values of various mean-squared internal distances (squared cell units) from $D(2)$ to $D(10)$ vs N (the number of chain beads), for a self-avoiding-walk chain (or for a polyelectrolyte chain at $\lambda=0$).

subsection. But from the slight increase with N of the first row of Table I, it can be observed that the influence of the excluded volume is larger when N gets larger, at this region of N.

It is important to stress that this investigation was carried out for $N \leq 64$. However, the general picture may look different for higher N.

The fluctuations of $D(n)$ increase with the increase of n. The subject of deviations is also interesting and requires further investigations.

I. Recent verification of the existence of physical statistical bonds in charged chains

Verification of the results of a computer model may be done in several ways: (a) comparison with real experiments; (b) comparison with analytic calculations; (c) self-consistency; (d) comparison with other computer modeling; and (e) changing physical conditions of the measured system and obtaining reasonable or meaningful results.

We therefore consider it of importance to compare ideas derived through our charged model to the ideas behind Table I and Eq. (3) in Kolinski and Skolnick's article [50], derived from a statistical analysis of a set of high-resolution three-dimensional (3D) structures present in the Brookhaven Protein Data Bank. The idea that there exist various potentials for various internal distances of the chain supports our claim that in the charged macromolecular system there exist a new type of physical statistical bonds (see the beginning of Sec. III and Refs. [25,34]). It also supports the main idea of this article that these statistical bonds vary with different internal distances. In this context, based also on results not yet published, we extend the existence of the new type of bonds to macromolecular systems of various types of charges.

IV. SUMMARY

One of the most important results of this study is the expansion of the new family of physical statistical bonds by the addition of another bond, the linear statistical bond. Various internal distances have different behavior when λ increases. That contacts and kinks are reduced was shown in previous articles. That linear bonds are increased is demonstrated in this article. The behavior of other bonds will be reported in the future.

Surprisingly, the kink fraction g, which was defined previously, has been found in this article [Eq. (7)] to be related to $D(2)$, the mean-square distance between the end beads of three adjacent beads. Local and global properties are therefore found to be connected. From the global size effect for g, detected previously, here we derive a local size effect in $D(2)$.

Additional meaning has been given to the kink fraction g in terms of the kink probability, defined as $1-P_l$, where P_l is the probability for a linear statistical bond. The average number of linear statistical bonds has been found to increase with increasing λ (Fig. 2), i.e., with temperature or dielectric constant decrease, or with increase of bead charge. The increase in the number of linear bonds with the increase of λ corresponds to the decrease of kinks with increasing λ. The increase stems from the connectivity of the polymer chain where disappearance of a kink must cause an increase in the number of linear bonds. The increase in the number of linear bonds along the chain has been examined. A new parameter P_{li}, the unkink probability for each group of three adjacent beads, has been defined. At $\lambda=0$ (SAW chain) all chain beads have been found to have the same value of P_{li}, except the ends, which have been found to be slightly more bent. At high λ, a vast difference has been found between the bent beads near the chain ends and the almost flat part in the middle of the chain (Sec. III C 3).

$D(3)$ has been also found to have a constant value at $\lambda=0$. More details about this will be reported in a future article.

The normalized internal mean-squared distance $D(n)/n^2$ at large values of n has been found to be more sensitive to changes in λ than at small values of n (Fig. 6). Thus, when the chain is free to choose its own shape as determined by the charge on its backbone, the changes due to physical conditions (expressed by λ) are small for short segments but very large for long segments. $D(n)/n^2$ has been suggested to be used as an inverse measure of segment flexibility.

The value of P_l and $\langle S^2 \rangle / \frac{1}{12}(N-1)^2$ has been found to be nearly equal, whereas P_{nc}, the probability of not

having a contact (defined in Sec. III E), has been found to have much higher values (Fig. 6). This means that $\langle S^2 \rangle$ appears to be influenced by the average number of linear bonds or of their complement, the average number of kinks ($\langle n_{\text{kink}} \rangle + \langle n_{\text{linear}} \rangle = N-2$), and not by the average number of contacts. A suggestion that a unique g is connected to the scaling has been raised. Empirical relations that connect the new parameters and the previously defined parameters have been found [Eqs. (10) and (11)].

End-to-end and internal mean-squared distances have been examined and the effect of the closeness of an internal distance to the chain end has been discussed (Sec. III H). In future work we will use internal distances to define additional new parameters that will increase the understanding of the unfolding mechanism.

Heuristic as well as numerical arguments have been given regarding the limitations on the applicability the blob concept (Secs. III C 2 and III C 4). The feeling that the blob picture is insufficient to explain chain expansion and that there must be some rules that describe the expansion was behind our new approach in polymer simulations. This approach, to describe the mechanism through which the macromolecule changes from a coil to a rod, was reported by one of us through the contact matrices but was considered even earlier in a nonmatrix form that will be reported in the future.

The expanding polyelectrolyte is a specific case of polymer expansion in general. The results of its investigation may be applicable to other cases. In future articles we plan to describe the preferred configurations in greater detail. We note here that the chain gets rid of those configurations with higher energy, yet tries to retain bend configurations since it costs entropy to lose them. The maneuvers made by the chain as λ increases is one of the subjects of our planned future articles.

ACKNOWLEDGMENTS

We thank the Bar-Ilan Research Foundation and C.B. thanks the Morris J. and Betty Kaplun Foundation for their support. We gratefully acknowledge the enlightening comments of Mr. David Bannett and stimulating discussions with Professor Jeffrey Skolnick.

[1] C. Brender, M. Lax, and S. Windwer, J. Chem. Phys. **74**, 2576 (1981).
[2] D. Bratko and V. Vlachy, Chem. Phys. Lett. **90**, 434 (1982).
[3] V. Vlachy and D. Dolar, J. Chem. Phys. **76**, 2010 (1982).
[4] C. Brender, Ph.D. thesis, Bar-Ilan University, 1982 (unpublished). In the thesis, the slithering snake off-lattice model for polyelectrolytes was developed.
[5] A. Baumgärtner, J. Phys. (Paris) Lett. **45**, L515 (1984).
[6] M. Le Bret and B. H. Zimm, Biopolymers **23**, 271 (1984).
[7] C. Brender, M. Lax, and S. Windwer, J. Chem. Phys. **80**, 886 (1984).
[8] R. Bacquet and P. J. Rossky, J. Phys. Chem. **88**, 2660 (1984).
[9] C. S. Murthy, R. J. Bacquet, and P. J. Rossky, and J. Phys. Chem. **89**, 701 (1985).
[10] P. Mills, C. F. Anderson, and M. T. Record, Jr., J. Phys. Chem. **89**, 3984 (1985).
[11] D. Bratko and V. Vlachy, Chem. Phys. Lett. **115**, 294 (1985).
[12] V. Vlachy and A. D. J. Haymet, J. Chem. Phys. **84**, 5874 (1986).
[13] J. M. Victor and J. P. Hansen, Europhys. Lett. **3**, 1161 (1987).
[14] (a) S. L. Carnie, G. A. Christos, and T. P. Creamer, J. Chem. Phys. **89**, 6484 (1988); (b) G. A. Christos and S. L. Carnie, *ibid.* **91**, 439 (1989).
[15] J. P. Valleau, Chem. Phys. **129**, 163 (1989).
[16] J. Takashima, M. Takasu, and Y. Hiwatari, Phys. Rev. A **40**, 2706 (1989).
[17] (a) C. Brender, J. Chem. Phys. **92**, 4468 (1990); (b) **93**, 2736 (1990).
[18] G. A. Christos and S. L. Carnie, J. Chem. Phys. **92**, 7661 (1990).
[19] H. H. Hooper, H. W. Blanch, and J. M. Prausnitz, Macromolecules **23**, 4820 (1990).
[20] H. H. Hooper, S. Beltran, A. P. Sassi, H. W. Blanch, and J. M. Prausnitz, J. Chem. Phys. **93**, 2715 (1990).
[21] C. Reed and W. Reed, J. Chem. Phys. **92**, 6916 (1990).
[22] G. A. Christos and S. L. Carnie, Chem. Phys. Lett. **172**, 249 (1990).
[23] M. Fixman, J. Chem. Phys. **92**, 6283 (1990).
[24] R. Penfold, S. Nordholm, B. Jönsson, and C. E. Woodward, J. Chem. Phys. **92**, 1915 (1990).
[25] C. Brender, J. Chem. Phys. **94**, 3213 (1991).
[26] P. G. Higgs and H. Orland, J. Chem. Phys. **95**, 4506 (1991).
[27] Y. Kantor and M. Kardar, Europhys. Lett. **14**, 421 (1991).
[28] Y. Kantor, Europhys. Lett. **14**, 767 (1991).
[29] C. W. Reed and W. F. Reed, J. Chem. Phys. **94**, 8479 (1991).
[30] C. E. Woodward and B. Jönsson, Chem. Phys. **155**, 207 (1991).
[31] C. E. Reed and W. F. Reed, J. Chem. Phys. **96**, 1609 (1992).
[32] H. L. Gordon and S. Goldman, J. Phys. Chem. **96**, 1921 (1992).
[33] C. Brender, J. Phys. Chem. **96**, 5553 (1992).
[34] C. Brender and M. Danino, J. Chem. Phys. **97**, 2119 (1992).
[35] C. E. Reed and W. F. Reed, J. Chem. Phys. **97**, 7766 (1992).
[36] A. Sassi, S. Beltran, H. H. Hooper, H. W. Blanch, and J. Prausnitz, J. Chem. Phys. **97**, 8767 (1992).
[37] J. L. Barrat and D. Boyer, J. Phys. (France) II **3**, 343 (1993).
[38] M. Severin, J. Chem. Phys. **99**, 628 (1993).
[39] F. Aguilera-Grania and R. Kikuchi, Physica A **189**, 108 (1992).
[40] F. Aguilera-Grania and R. Kikuchi, Physica A **195**, 53 (1993).
[41] R. Penfold, B. Jönsson, and S. Nordholm, J. Chem. Phys. **99**, 497 (1993).
[42] P. Y. Lai and K. Binder, J. Chem. Phys. **98**, 2366 (1993).

[43] The values of g in Table III are similar to those published by us in Fig. 8 of Ref. [34], but not identical. They are slightly greater, especially for low N and at high λ. Thus one can use Eq. (2) of Ref. [34] only as an estimate for the average number of kinks. More precise results are obtained by a direct counting of the number of kinks. The use of $\langle n_{\text{kink}} \rangle + \langle n_{\text{linear}} \rangle$ instead of $N-2$ in the expression for g gives slightly improved results, probably because of error cancellation.

[44] P. G. de Gennes, *Scaling Concepts in Polymer Physics* (Cornell University Press, Ithaca, NY, 1985).

[45] P. G. de Gennes, *Simple Views on Condensed Matter* (World Scientific, Singapore, 1992).

[46] P. G. de Gennes, P. Pincus, R. M. Velasco, and F. Brochard, J. Phys. (Paris) **37**, 1461 (1976).

[47] Y. Rabin, J. Chem. Phys. **88**, 4014 (1988).

[48] C. Brender (unpublished).

[49] C. Brender (unpublished).

[50] A. Kolinski and J. Skolnick, J. Chem. Phys. **97**, 9412 (1992).